











Recent Advances and Future Directions in Imaging of Peripheral Nervous System: A Comprehensive Review for Therapeutics Approach

Mehran Ebrahimi Shah-abadi¹ , Armin Ariaei² , Hossein Mohammadi³ , Arash Shabani⁴ ,
Rastegar Rahmani Tanha⁵ , Vahid Tavakolian Ferdousie⁶ , Abdolmajid Taheri⁷ ,
Mohsen Marzban⁸ , Mahdi Heydari⁹ , Auob Rustamzadeh^{10*} 

1. Dept. of Surgery, Afzalipour Hospital, Kerman University of Medical Sciences, Kerman, Iran
2. Student Research Committee, School of Medicine, Iran University of Medical Sciences, Tehran, Iran
3. Dept. of Bioimaging, School of Advanced Technologies in Medicine, Isfahan University of Medical Sciences (MUI), Isfahan, Iran
4. Dept. of Radiological Sciences, Faculty of Allied Medicine, Iran University of Medical Sciences, Tehran, Iran
5. Dept. of Neurosurgery, School of Medicine, Imam Reza Hospital, Kermanshah University of Medical Sciences, Kermanshah, Iran
6. Dept. of Neurosurgery, Bahonar Hospital, Kerman University of Medical Sciences, Kerman, Iran
7. Dept. of Radiology, Faculty of Medicine, Shahrekord University of Medical Sciences, Shahrekord, Iran
8. Student Research Committee, Iranshahr University of Medical Sciences, Iranshahr, Iran
9. Dept. of Anatomical Sciences, School of Medicine, Jiroft University of Medical Sciences, Jiroft, Iran
10. Dept. of Anatomy, School of Medicine, Iran University of Medical Sciences, Tehran, Iran

Article Info

 [10.30699/jambs.31.148.415](https://doi.org/10.30699/jambs.31.148.415)

Received: 2023/02/16;

Accepted: 2023/06/20;

Published Online: 29 Oct 2023;

Use your device to scan and read the article online



Corresponding Information:

Auob Rustamzadeh,

Dept. of Anatomy, School of Medicine,
Iran University of Medical Sciences,
Tehran, Iran

E-Mail:

auob2020rustamzade@gmail.com

ABSTRACT

PNS (Peripheral nervous system) disease comprises a wide range of manifestations from acruable damage to nerve body degeneration. Finding proper imaging sequences of MRI (Magnetic Resonance Imaging) to maximize the detection sensitivity and specificity of PNS injuries, is the purpose for which this study was conducted. In this regard, due to Wallerian degeneration, axonal degeneration and inflammation after nerve injury, were mentioned as the inseparable factors of nerve damage, and clues to be detected by the MRI. Gadofluorine M and USPIO nanoparticles are candidates which provide contrast in multiple aspects, such as diagnostic approaches and drug tracking. For instance, the P904 USPIO particle is proper for long-term monitoring, while the CS015 (PAA-coated USPIO), USPIO-PEG-tLyP-1, and USPIO nanovesicles are appropriate for drug delivery. Besides contrast agents, the implication of gradient echo or 3D DW-PSIF provides more precious data over conventional sequences, including T2-weighted on the physiological or pathological PNS status. Eventually, although the real-time imaging and simplified procedure of the ultrasound technique have advantages over MRI, the low-resolution disvalues its benefits. Alternatively, there is a growing trend in the application of Diffusion-weighted imaging (DWI) to acquire a clear concept of disease diagnosis, along with Diffusion tensor imaging (DTI) to successfully monitor the rate of nerve regeneration that is applicable for therapeutic approaches.

Keywords: PNS, MRI, Ultrasound, Nanoparticle, Nerve Regeneration

Introduction

Neuropathy is a nerve injury that can lead to sensory A complicated web of neurons located outside the central nervous system (CNS) with intricate interaction of synapses, is known as the Peripheral nervous system (PNS). The PNS mainly consists of ganglions, sensory and motor neurons, and multiple synaptic junctions (1). This system acts as a bridge for transferring bilateral

signals from external stimuli to CNS and reverses the signals through cranial (originated from the brain stem and forebrain), ventral, and dorsal (originated from the spinal cord) nerves. The ventral (motor axons) and dorsal (sensory axons) roots divide just next to the intervertebral foramina to innervate different parts of the body in a pattern in which the posterior (dorsal) supplies muscles

and skin of the back, whereas the anterior (ventral) ramus is limited to limb muscles and the skin of the ventral part of the body. Subsequently, they are divided into smaller branches to innervate each muscle (2). Each division of these fibers may be supported by a myelin sheath or lack it. Besides, endoneurium, a specific connective tissue, surrounds axons. Since axons have close connectivity with each other before innervating targeted muscle fibers, another connective tissue layer is needed to support the structure of bundles known as perineurium. Besides its supportive role, this layer acts similar to the pia-arachnoid layer of the spinal cord, by providing blood-barrier properties for the axons (3). Moreover, protection of the nerve bundles can be supplemented by another layer containing dense connective tissue with larger diametral supports, named epineurium (4). Finally, two additional layers still exist, one with loose connective tissue outside of the epineurium and the other one with loose areolar connective tissue attributes, known as mesoneurium (5). The particular morphology of the PNS is a basis on which imaging techniques were manipulated to specify the PNS from adjacent tissues. Contrast agents are appropriate particles to differentiate PNS from similar tissue structures. Contrast agents are made of Fe particles with multiple limitations such as self-adhesion and low stability within in vivo conditions (6). As a compensation, there is a suggestion to utilize a combination of gold nanoparticles and Fe to boost the stability and signal quality of the tissue. Gold nanoparticles were formerly applied for therapeutic approaches that targeted tumors (7-9). Nevertheless, there are multiple obstacles, including determination of the optimum size of the nanoparticles and eliminating the unpredicted hazardous property of them (10, 11). Unfortunately, up to now, a comprehensive review article comprised of the traditional and novel imaging techniques, which introduces the applicable imaging sequences in PNS imaging, has not been conducted. Moreover, the role of USPIO and nanoparticles in enhancing the quality of PNS imaging has been neglected. This study aimed to present proper imaging methods and devices for visualizing the PNS anatomy accurately, in order to provide an appropriate background for the specialists to make a better diagnosis.

Materials and Methods

PubMed and Science Direct. In addition, a list of keywords was chosen to search specifically in the keyword, title, and abstract part of each article. At first, an advanced search option with the search query of ((peripheral AND nerve) AND (morphology AND injury)) was performed in Science Direct and PubMed databases in the title, abstract, and keywords, with a total number of 322 and 313 results, respectively. There was no specific restriction on the year of publication, whereas there was an attempt to select the most recent articles in case of finding similar concepts. The inclusion criteria were: providing a clear explanation, novelty and validity of the explained subject, and peer review journal. To introduce peripheral nerve and related diseases, a total number of 17 articles, which provide a clear explanation

of the anatomy of the PNS, were selected. A similar search strategy was performed for the USPIO nanoparticle, with the search query (USPIO AND nanoparticle AND imaging). The search result was disclosed with 81 and 75 articles in Science Direct and PubMed, respectively. A total number of six most recent and two complementary original articles were selected to fill in the data of Table 1. Moreover, four articles were fitted properly to introduce the subject. Finally, to find and scrutinize magnetic resonance imaging techniques, a search query comprised of ((MRI AND imaging) AND (peripheral AND nerve)) was applied considering high quality, low standard error, and relativity to nerve injury detection. Six original DTI articles along with four original DWI articles were included in the study, by which Table 2 was filled.

Results

Nerve injury

Schwann cells have a vital role in myelin sheath formation along with conducting injured nerve axons to grow in a proper direction. After the nerve injury, there is a disruption in the axonal flow, resulting in axonal and myelin degradation due to the lack of energy support, nominated as Wallerian degeneration (12). Although there are different types of nerve damage from partial axonal damage to an unrecoverable cell body loss (13), all injuries are highlighted by inflammation and tissue clearance commenced by macrophages, as an inseparable post-traumatic compound (14). In this phenomenon, chemokines and cytokines are the mediator of cell signaling, in a way that neutrophils utilize them to attract macrophages derived from blood or resident monocytes, to the target area to infiltrate the nerve (15). Besides the devastating action of macrophages, they can involve in neuron regeneration by implementing two primary duties. One of them is neovasculature formation, and the other is helping Schwann cells to align in the correct direction for axonal growth (16). To perform this procedure, macrophages produce several growth factors like Brain-Derived Neurotrophic Factor (BDNF) (17), which could accelerate Schwann cells' maturation after nerve injury (18). During the retrieval of a peripheral nerve, if the Schwann cells migration fails to be implemented in the accurate line, or an inflammation occurs as a result of external long-term pressure, chronic pains may appear which could reduce the life quality of patients. Sometimes nerve recovery becomes impossible due to the high-intensity of the damage. In these conditions, we could apply two surgical techniques named neurolysis and neuroorrhaphy.

In the Neurolysis method, chronic pain is alleviated by cutting the specific part of the nerve, implemented by neurosurgeons (19, 20). This method has positive results in patients who are suffering from carpal or peroneal tunnel syndrome in the case of ligament entrapment or Osteotendinous (21). By applying this method, nerve regeneration initiates, and after a while, the same

condition as before treatment intervention, appears. In this case, to prolong the nerve recovery period, chemical substrates such as ethanol and ^{125}I radioactive seed are administered to the targeted area, (22). The second method called Neurorrhaphy is mainly used for the facial nerve, in which the disjoint fiber attaches to its neighboring nerve (23). This method was reported to restore muscle ability for contraction, in patients with flaccid or non-flaccid facial palsy (24). Advanced imaging techniques can be an applicable tool to monitor and follow up on the efficiency of therapeutic methods in order to establish a proper treatment strategy.

Imaging related nanoparticle

Ultrasmall superparamagnetic particles of iron oxide (USPIO) nanoparticles are supplementary agents used in imaging research procedures, due to their low involvement in cellular reactions and high biocompatibility (25, 26). The USPIO nanoparticle or Iron oxide nanoparticles (IONs) consist of two main parts: A sheathing part containing organic compounds to protect the internal part, which commonly has a 4 to 10-nm diameter core of magnetite (Fe_3O_4) or maghemite ($\gamma\text{-Fe}_2\text{O}_3$ or $\alpha\text{-Fe}_2\text{O}_3$) (27). As previously mentioned, among the advantages of this compound is its safety, which is justified in Maraloiu *et al.* research. In their study, P904 USPIOs were injected into mice to evaluate the atherosclerotic plaques. The results illustrated a nontoxicity property of P904 USPIOs in maghemite (Fe^{3+}) form, even by increasing the dosage. In addition, the researcher claimed that in the preclinical studies, prescribing dose of 12 millimoles Fe/kg wt represented no toxicity. The study employed advanced techniques, including Two-Photon Laser Scanning Microscopy (TPLSM) and High-Resolution Transmission Electron Microscopy (HRTEM) to assess atherosclerotic plaque. The USPIOs provided effective magnetic contrast agents to execute *in vivo* TPLSM method. Nevertheless, this method has a penetrating limitation through gross tissue. Instead, utilizing nonlinear micro-endoscopy in the study of thick tissue, is applicable. In addition, some of the USPIO nanoparticles encountered phagolysosomal processing, in which the maghemite core changed to ferritin form, resulting in long-term storage (28). Although previous research administrates high doses of USPIO nanoparticles, it is possible to get sufficient signals from tissue with much lower doses. In a study conducted by Oghabian *et al.*, the threshold dose to obtain proper contrast of lymph nodes was defined in the rat. The results clearly depicted that subcutaneous injection (0.028 mg Fe/kg) demands a much lower dose than intravenous injection (0.16 mg Fe/kg) (29). This data suggested that the subcutaneous injection method maximizes the effectiveness of obtaining images from different tissues, since the excretion rate decreased.

Moreover, ten years after Oghabian *et al.* research, Nie and colleagues conducted a similar study with another form of USPIO nanoparticles called CS015. This nanoparticle has more advantages than the previous one, including a Poly Acrylic Acid (PAA) surface which provides multiple loading sites for drug delivery and drug tracking, even though some portions of them are endocytosed by tissue-resident macrophages. By utilizing Magnetic resonance (MR) lymphangiography to specify the CS015, similar to previous studies, there is an assumption on the priority of subcutaneous injection over intravenous injection (30). Based on the peripheral nerve structure, one of the challenging issues in detecting, especially in large nerve trunks, is the perineurium layer, which acts as a blood barrier. In a recent animal study, Wu *et al.* used a modified form of USPIO nanoparticle called USPIO-PEG-tLyP-1 which can cross the blood-brain barrier. The aim of developing this particle was to disclose tumor tissue because of its high binding affinity to neuropilin-1. Using an MRI system, the particle could easily be tracked, suggesting it as a potential candidate for glioma detection, as well as other research purposes like peripheral nerve imaging (31).

In another research, the USPIO was reorganized by Cy5.5 and PEG in order to construct a new probe, named USPIO-PEG-Cy5.5. The particle revealed relatively high stability and biocompatibility along with a wide excitation wavelength (32). Another advantage of USPIO nanoparticles is tracking either resident cells with no migration or mobile cells, in blood and tissue. This phenomenon helps researchers detect nerve inflammation with high efficiency. An *in-vitro* research on chimeric antigen receptors (CAR) T cells illustrated a new method in which immune cells could be signed. In this way, every tiny inflammatory site in the body could be detected through the MRI (33). It is also possible to adjust the USPIO nanoparticle to the morphological traits of the targeted tissue. In this regard, a specific sequence of peptides is conjugated with PEG-coated USPIO to make it adaptive to the brown adipose tissue (BAT). The particle could specifically bind to the targeted tissue to estimate the volume of the targeted area by the MRI (34). Finally, it is important to mention the role of the USPIO in tracking drug delivery. Tracking the effectiveness of drug delivery has a remarkable role in following up the patients who suffer from cancer. In addition to cancer, there is a possibility to study a wide range of diseases including peripheral nerve injuries. In animal research, the chemotherapeutic drugs with the admixture of the USPIO nanovesicles were employed to define the fate of the drug by the MRI (35) (Table 1).

Table 1. The USPIO nanoparticle's role in disease detection and therapeutic purpose

Study	Target	Nanoparticle type	Method	Type of Research	Highlighted
Maraloiu, V.A. et al 2016 (28)	atherosclerotic plaques	P904 USPIO	Two-Photon Laser Scanning Microscopy (TPLSM) and electron microscopy	In vivo - ApoE ^{-/-} mice	No dose-dependent adverse effect safety long time monitoring
Oghabian M.A. et al 2010 (29)	lymph nodes	Nanomag-D-sprio nanoparticles	1.5 T subcutaneously (the dorsal portion of the left front paw of rats) and intravenously injection tracking 24 hours after injection	In vivo-rat	More sensitivity of gradient echo (GRE) sequences to susceptibility artifact than spin echo (SE) sequences Lack of refocusing pulses in GRE sequences. 0.16 mg Fe/kg for intravenous and 0.028 mg Fe/kg subcutaneous injection for a minimum dose
Nie Y., et al 2020 (30)	lymph nodes	CS015 (PAA-coated USPIO)	1.41T NMR spectrometer Atomic absorption spectrometry (AAS) Origin 9.1 calculated iron concentration	In vivo-Female SD rats	providing a large number of loading sites drug delivery target promising MR contrast agent
Wu W., et al 2020 (31)	neuropilin-1 (NRP-1) from human glioma U87 cell line	USPIO-PEG-tLyP-1	7.0 T Scanning after 6h, 12 h, and 24h T2WI sequence: TR = 3500 ms, TE = 72 ms, FOV = 400mm, layer thickness 1.00 mm, layer spacing 0.5 mm, matrix 256 × 256 T ₂ map sequence TR = 1562 ms, TE = 9 ms, FOV = 400mm, layer thickness 1.00 mm, layer spacing 0.5 mm, matrix 256×256	In vivo-nude mice	Penetrating the blood-brain barrier (BBB), High binding affinity to NRP-1
Liu Q. et al 2022 (32)	Thyroid cancer cell line	USPIO-PEG-Cy5.5	SF (MHz): 21, O1 (Hz): 569335.95, P1 (US): 14.00, Td: 29994, PRG:1, TW(ms): 300.000, P2(us): 29.00, TE(ms): 0.300, NECH: 1000, NS: 8	In vitro	Low toxicity, wide excitation wavelength, good stability, and biocompatibility
Xie T., et al 2021 (33)	chimeric antigen	the amino alcohol derivatives of glucose-coated	7.0 T magnetic resonance imaging	In vitro	Tracking CAR T cells,

Study	Target	Nanoparticle type	Method	Type of Research	Highlighted
	receptors (CAR) T cells	nanoparticles, ultra-small superparamagnetic particles of iron oxide (USPIOs)			Evaluate therapeutic effects,
Hu Q., et al 2021 (34)	brown adipose tissue (BAT)	The peptide was conjugated with PEG-coated USPIO	T2*-weighted images	In vivo- Male C57BL/6 J mice	Measuring brown adipose tissue activity
Liu D., et al 2020 (35)	Tumor cell	USPIO nanovesicles	7 T The multi-slice T1 MRI RARE sequence using the following parameters: Repetition Time = 350 ms, Echo Time = 10.3 ms, Effective TE = 10.3 ms, Rare Factor = 2, Flip Angle = 180.	In vivo- HCT116 mouse tumor model	Drug tracking Disease prognosis

Imaging techniques

In the clinical approach, Ultrasound and Magnetic resonance imaging (MRI) are conducted to take images of the PNS. Physicians mainly prefer to use ultrasound for their diagnostic aims, especially for tumor and entrapment syndromes, since it has lower cost and takes less time than MRI, while MRI still depicts a growth potential for experimental goals. It provides substantial information across the body with multiplanar abilities and high contrast resolution (1). In the following, multiple sequences and techniques of the MRI application are stated to help characterize the proper method in PNS imaging.

Conventional MRI

In the MRI technique, multiple sequences are available to obtain signals from the targeted area. In this section, conventional MRI sequences are compared to each other, to state the suitable method for peripheral nerve imaging. By utilizing T1-weighted spin-echo sequences, it can be possible to assess morphological properties along with high spatial resolution. Moreover, T2-weighted spin-echo sequences, are commonly employed to gain information on tissue, due to proper contrast resolution (36). To acquire detailed data about inflammatory diseases or even tumors, it is noteworthy to set long echo times of MRI, usually 100 ms, to take highly weighted T2 sequences. In addition, two to four-millimeter sections are required to set the spatial resolution at maximum value. These settings are used in combination with fat signal suppression, which is implemented by spin-echo (SE) or turbo spin-echo (TSE) sequences. Sometimes Short Tau Inversion Recovery (STIR) or T1 weighted sequences associated with gadolinium injection are a substitute for the

previous method (37, 38). One of the challenges in T1 weighted sequences is the isointense signals of the nerves compared to the muscles. In this case, one of the ways to distinguish peripheral nerve is epineural fat, characterized by a hyperintense halo (39). On the contrary, by applying T2 weighted sequences, nerves appear somehow hyperintense with even higher intensity in large nerve trunks fascicles, mainly because of endoneurial fluid (36).

Yet, studies imply that MRI is the first candidate for nerve damage diagnostic approaches. In Mulkey et al. study, there was an increase in the cauda equina nerve root diameter, which was a diagnostic clue to detect inflammatory polyneuropathies (40). In T2 weighted sequences with or without fat suppression, detecting possible fascicular damages becomes possible and by applying gadolinium injection in T1 weighted sequences, some branches of the blood-nerve barrier could even be tracked (1). To evaluate the existence of Wallerian degeneration in the damage site, the T2 weighted sequences can be suitable (41). It generally requires a minimum of 24-hour interval to highlight a clear hyperintensity in signal illustration, after the injury happens (42). After a 48 hours interval, while the morphology properties of adjacent tissue depict a normal status like muscles, in T2 weighted sequences there is a clear wide hyperintensity defined as edema condition (43). In the final stage, in which the adjacent muscles suffer from denervation, their amyotrophic stage initiates, detected by a hyperintense T1 signal accompanied by long-time denervation persistence (44). Nevertheless, one of the challenges in conventional MRI is acquiring high-quality images to differentiate peripheral nerves from vessels, due to the same diameter and signal intensity in T2-weighted sequences. Even T2 weighted spectral adiabatic inversion recovery turbo spin echo (T2 SPAIR TSE)

sequences, despite their high resolution, cannot differentiate two structures (45, 46). One of the suggested methods to define peripheral nerve is to put focus on normal or damaged nerve fascicular layer, through peri-mural and intra-mural fat (47).

Three-Dimensional Diffusion-Weighted PSIF (3D DW-PSIF)

Besides the mentioned techniques, MRI can obtain 3D volume data of the sample. By using this method, complex nerve pathways, such as the brachial plexus, could be analyzed with higher efficiency, since the neurography contains satisfying isotropic quality with curvilinear multiplanar reconstructions. Moreover, the physician could track the efficiency of treatment by applying Maximum intensity projection (MIP) (48, 49). Three-Dimensional Diffusion-Weighted PSIF Technique (3D DW-PSIF) provides a large field of view (FOV) and proper shimming, while some areas may reflect ghosting artifacts. Nonetheless, 3D DW-PSIF still provides high conspicuity scores compared to T2 weighted images (1.57 ± 0.67 versus 0.74 ± 0.76), when applied to peripheral nerves including: lumbosacral plexus, brachial plexus, and sciatic nerve. This MRI method offers more data and provides a more accurate diagnosis of pathological nerve conditions (50).

Gadofluorine M contrast agent

Another MRI technique for obtaining high-quality images of peripheral nerve, is using contrast agents. In novel animal research, a significant increase in signal intensity was observed among rats that took Gadofluorine M contrast agents for sciatic nerve data acquisition. By applying contrast agents, the reconstruction and retrieving stage of the peripheral nerve could be assessed. Strengthening the signal amplitude allows physicians to have deep insight into disease progression, along with justifying the clinical symptoms with the predicted illness, whereas contrast agents lack the ability to be applied in a wide range of nerve damages. For instance, Gadofluorine M can only reveal the inflammatory aspect of nerve lesions (51). Former research utilizes Gadofluorine M, similar to the USPIO, as a sign of the degeneration process triggered by macrophages, since it could bind to myelin-degraded particles (52, 53). Moreover, Gadofluorine M was reported to have the potential to detect several nerve damages, including demyelination and Wallerian degeneration. Regarding this fact that in the nerve injury process, the signal intensity is concentrated in the damaged area, it can be concluded that the blood-nerve barrier is responsible for the high influx of Gadofluorine M, reaching for the nerves (54-56).

Functional magnetic resonance imaging (fMRI)

It is noteworthy to mention a well-known MRI technique named Blood-oxygen-level-dependent (BOLD) fMRI and its application in peripheral nerve imaging. This method has a powerful ability to record brain function, in which there is facilitation in

monitoring myelinated axonal activity for multiple aims, ranging from basic psychological research to clinical approaches. Its limitation in employment on gray matter tissue, makes it suitable to exclude unwanted signals, in peripheral nerve imaging. It was successfully implemented on bullfrog sciatic nerves to evaluate and visualize axonal stimulation. Diffusional fMRI also participates in the detection of microstructural changes occurred in myelin fiber, which are linearly correlated with electrical impulses (57). Besides mentioned methods and techniques, we could consider more specific methods in which detailed information could be obtained about the quality of fibers in nerve function, and possible denervation without any sign of inflammation (58). One of these methods is nominated as Diffusion-weighted imaging (DWI) which is mentioned in the following section.

Diffusion-weighted imaging (DWI)

The DWI is based on the key compound in biological processes called water molecules, in which quantitative data are obtained from tracking its movement (59). The different behavior of water molecules in the tissue encountered pathological conditions, results in significant differences in signal intensity of normal and damaged tissue (60). In human research conducted on a tiny sample size of five participants, Diffusion-weighted MR neurography (DW-MRN) sequences, based on DWI, were obtained to scrutinize the sacral plexus. The results defined a concept of the priority of unidirectional MPGs in peripheral nerve image acquisition. Moreover, utilizing soap-bubble MIP depicts better results in gaining detailed information compared to the conventional MIP method (61). While in the previous research, the small sample size is the overt limitation that decreases the reliability of the results, in another study with a larger sample size (N=65), the head and neck of the participants were evaluated with different methods of DWI. As the data illustrated, Multishot EPI spectral presaturation with inversion recovery (msEPI-SPIR) is superior to single-shot EPI (ssEPI), since it contains higher image quality and provides fewer artifacts. In the DWI neurography, massive fat suppression results in an increase in signal-to-noise ratio (SNR) as well as apparent diffusion coefficient (ADC) improvement (62). Although the previous study mainly focused on the central nervous system (CNS), Takahara et al.'s study on peripheral nerve injury, showed that DW-MR neurography could be considered as a suitable method for localizing nerve injury and determining the type of the disease (58, 63) (Table 2). Finally, in the most recent research conducted by Koike et al. in patients with malignant peripheral nerve sheath tumor (MPNST) and plexiform neurofibroma (pNF), the result of the study recommended the DWI method in discriminating these two diseases. Moreover, the combination of Wasa's score and ADC map is suggested to be implemented to increase the accuracy of diagnosis (64). In the next section, another well-known technique for gathering

data on peripheral nerves, named Diffusion tensor imaging (DTI), is scrutinized.

Diffusion tensor imaging (DTI)

In the DTI technique similar to Diffusion tensor imaging (DWI), image analysis is based on water molecules. In Haakma *et al.* research, a three-tesla magnetic field is utilized to acquire a 3D image of the sacral plexus with a sample size of ten patients. The result is depicted by detailed information across the L4-L3 area of the participants. By scrutinizing the study result, it could be perceived that S1 in the mean diffusivity (MD) and Radial Diffusivity (RD) parameters have a meaningful alternation in comparison to normal and patients, while L4 and L5 were not depicted at any significant rate. Based on the results, The MD parameter could be considered as an accurate parameter in the detection of PNS pathological states. Since this method of MRI is rarely implemented in clinical studies to finally, the study suggested using a combination of methods, including the 3D Turbo spin echo (3D-TSE), DTI, and Fiber tractography (FT) (65). One way to increase the confidential ratio of the image acquisition to determine what happened during nerve injury, is increasing the magnetic field strength (MFS). In recent animal research, the sciatic nerve of rats was put into focus. Animals were divided into three groups, sham, crush, and cut. All groups were taken on DTI imaging techniques with 7 T MFS. The data collection was based on a specific timeline to define the most suitable time for nerve injury detection. The results suggested that a four weeks interval was the best for distinguishing between multiple nerve injury types. This issue is mainly because of the influence of inflammation. After four weeks, the inflammation dwindles, then the nerve begins to regenerate. Moreover, in this condition, in which proximal nerves are involved, the golden time for detection becomes even shorter, compared to distal nerves. In this study, unlike the previous one, the researcher suggested the FA parameter for nerve injury detection. In transection cut at one and 4 weeks after injury, a remarkable reduction in FA parameter could be revealed (66). By measuring FA over time, an overall period of 12 weeks for complete recovery, could be conclude. Nevertheless, the main challenge of image distortion still remains and even exacerbates with higher MFS. To cope with the unpleasant issue of artifacts and distortion which are mainly due to B0 inhomogeneity as well as eddy currents, in a human study, the author suggested a method named TOPUP for image recovery. This study was conducted on humans with 7 T MFS to obtain detailed information on the peripheral nerve of the arm and carpal tunnel, by utilizing the Steady-state free precession MRI (SSFP) sequence to minimize the slice thickness to 0.2 x 0.2mm and 0.4 mm. With the aid of this method, several structures of the peripheral nerve could be visualized, including

single fascicles of the median nerve, branches of the superficial radial nerve, and the sheaths of the flexor tendons. Nevertheless, there are particular difficulties, especially with high MFS, including low spatial resolution when the echo-planar (EPI) method is performed for image acquisition, which leads to less assurance to discern peripheral nerve compounds. Besides, the DTI method has the potential to diagnose neuropathies with an entanglement of small-diameter trunks. Similar to Farinas *et al.* (2020), Schmid *et al.* (2018) study revealed FA as the most proper parameter for peripheral nerve imaging. Finally, the time-consuming procedure to acquire proper signal ratio images, remains the major challenge for high MFS applications (67).

Formerly, DTI was one of the methods to assess white matter integrity, with reliable implementation in the demonstration of inflammation or possible edema (68). A similar methodology can be applied to the peripheral nerve to evaluate the type of injury and treatment rate. It is worthy to indicate the contrary attitude of FA and RD in the diagnosis of nerve injury, in which reduced FA is illustrated as a clue for myelin and axon degeneration while an increase in RD could be concluded as the same result, however, RD is not recommended for nerve injury prognosis. In these two studies, first, Sun *et al.* conducted animal research on rabbits with 1.5 T MFS in healthy and nerve injury model groups. The data suggested approximately 10 weeks for nerve recovery, detected by FA (69). Secondly, Yamasaki *et al.* collected data over time from the sciatic nerve injury model of rabbits, which found significant changes in FA during the second and fourth week after the injury. In this research, a more powerful MFS (7 T) is utilized compared to previous research (70). In another research, all the DTI parameters were compared to each other in order to clarify the most sensitive parameter in nerve injury diagnosis, in which by the aid of 3 T MFS, numerous data across the median nerve was obtained. The results highlighted FA and RD as an appropriate indicator of the quality of myelin sheath. However, FA could indicate the myelin sheath integrity better. Among other parameters, MD lacks the minimum criteria to be considered as a diagnostic value, while AD could still be perceived as an additional data provider for the RD and FA. The pros of this method compared to other sequences of MRI, is its ability to provide detailed data on the nerve, by which we could detect small lesions in peripheral nerves and even peripheral neuropathies (71). Eventually, it is noteworthy to briefly mention that the Diffusion basis spectrum imaging (DBSI) method could provide a larger amount of data compared to DTI, even though still the DTI data acquisition produces enough information on the condition of the peripheral nerve (57) (Table 2) (Figure1).

Table 2. Implementation of DTI and DWI in clinical and animal research

Study	Target area	Nerve injury model	Method	Type of Research	Magnetic field strength	Highlighted	Data
Haakma W., et al 2014 (65)	sacral plexus	Spina bifida	DTI	In vivo - Human	3 T	subject geometric and motion distortions identify nerve abnormalities the best performance in the MD parameter	N=10 Group1: 1.83±0.24 N:10 Group2: 1.40±0.22 P<0.001
Farinas AF., et al 2020 (66)	Sciatic nerve	3 cm longitudinal incision	DTI TE/TR of 22/425ms, FOV of 60×60×160mm	In vivo-rat	7 T	Interval of 4 weeks for distinguishing	crush=23, cut/ regeneration=19 mean crush=0.08 mean cut=0.15 p<0.05
Schmid A.B., et al 2018 (67)	Arm, forearm, carpal, and metacarpal	Neuropathies	DTI Echo time: 3.11 ms Field of view: 100mm Bandwidth: 349 Hz/Px voxel volume (0.2 x 0.2mm, 0.4-mm slice thickness)	In vivo-human	7 T	Visualization of single fascicles of the median nerve, branches of superficial radial nerve, and the sheaths of the flexor tendons. Detecting neuropathies	N=6+8 [95% confidence intervals]: FA, 0.955 [0.860–0.986]; MD, 0.867 [0.586–0.957]; P < 0.0001
Sun C., et al 2014 (69)	Sciatic Nerve	Nerve crush using a 16-cm needle forceps	DTI TR/TE: 8184/66 milliseconds, b = 1000 s/mm ² , slice thickness 1.6 mm, gap 0 mm, field of view: 130 mm, matrix 80 × 80, in-plane pixel size: 1.6 × 1.6 mm	In vivo-rabbits	1.5 T	FA parameter has a significant positive correlation with functional recovery,	N=32 FA ₁ : 0.4 FA ₂ : 0.51 P<0.05
Yamasaki T., et al 2015 (70)	Sciatic Nerve	Ligation	DTI repetition time, 3 seconds; effective echo time, 26 ms;	In vivo-rabbit	7 T	FA is useful in the prognosis of motor function after damaging	N=3 FA ₁ : 0.39 ± 0.01

Study	Target area	Nerve injury model	Method	Type of Research	Magnetic field strength	Highlighted	Data
			echo train length, 4; echo space, 9.8 ms; FOV:100×100 mm; pixel matrix: 128 × 128; slice thickness, 2 mm; numbers of average, 4; B-value: 0 and 700 s/mm ² .			the peripheral nerve	FA ₂ : 0.355 ± 0.01
Heckel A., et al 2015 (71)	median nerve	Healthy subject	DTI TR 3800 ms, TE 99 ms, b-value 0 and 1200 s/mm ² (encoded in monopolar 19 directions), readout bandwidth 1395 Hz/px, 18 slices, interslice gap 1.2 mm, FoV 150 x 150 mm ²	In vivo-human	3 T	FA and RD as a proper indicator of the quality of myelin sheath FA could better indicate the myelin sheath integrity	N=30 FA: 0.54±0.07 RD: 0.84±0.16
Takahara T, et al 2010 (61)	sacral plexus	Healthy subject	DWI Sequence: Single-shot EPI Acquisition plane: Axial FOV (mm): 350 Rectangular FOV percentage: 80% TR/ TI/ TE (ms): 12,664/250/80 Slice thickness/gap (mm): 4/0 (overlap) B-value (s/mm ²): 800	In vivo-human	3 T	DW MRN with unidirectional MPGs depict better images of the sacral plexus that three-directional or six-directional MPGs of DW MRN	N=5 Group1: 2.22 ± 1.04 Group2: 1.71 ± 1.06 Group3: 1.76 ± 1.05 Group4: 1.41 ± 1.02 Group5: 0.99 ± 0.76 Group6: 1.00 ± 0.81
Bae YJ., et al 2018 (62)	Head and neck	Tumor	DWI b-values: 0 and 1000 s/mm ²	In vivo-human	3 T	Obtaining high-quality images with msEPI-SPIR Fewer artifacts	N= 65 4.45 ± 0.84 7.69 ± 1.90

Study	Target area	Nerve injury model	Method	Type of Research	Magnetic field strength	Highlighted	Data
			single-shot EPI-STIR, single-shot EPI-spectral presaturation with inversion recovery,			Less image distortion compared to the ssEPI sequences, Higher CNR compared with ssEPI-STIR and/or ssEPI-SPiR.	
			DWI maximum gradient strength: 33 mT/m FOV: 128 × 160			A high-quality image of the brachial plexus with discriminating small nerves	N=5
Takahara T., et al 2008 (63)	brachial plexus	lesions	half-Fourier factor: 0.6 echo-planar imaging factor: 47 b value: 1000 sec/mm ²	In vivo-human	1.5 T	DW MR neurography helps to localize the damaged area of the brachial plexus	Not available
			DWI b value = 0 and 800 or 1000			Discriminate MPNST and pNF High accuracy by using Wasa's score and ADC map	N=10, 19 - ADC mean= 2.06-3 mm ² /second P-value 0.03
Koike H., et al 2022 (64)	Peripheral Nerve Sheath	MPNST and pNF		In vivo-human	Not mentioned		

Computed tomography (CT) scan

There is a wide range of methods for nerve disease diagnosis, which two of them commonly utilized in clinical approaches, are computed tomography (CT) scan and ultrasonic sound. The CT scan similar to the MRI, has a high spatial resolution in which different tissues take different contrasts (72). Hence, tiny lesions as well as nerve tumors, can be detected in the peripheral nerves (73). Furthermore, spinal nerve compression status known as intraforaminal, extraforaminal, and intradural, along with type 1 neurofibromatosis, can be easily detected (74-76). Nevertheless, this method unlike DTI, has a limitation in detecting and tracking nerve microstructural changes, mainly due to inadequate contrast resolution (77).

Ultrasound (US)

Similar to DWI in the ultrasound method some nerve injuries like MPNST and benign peripheral nerve

sheath tumors (BPNSTs), could be detected (78). In animal research on rabbits, the sciatic nerve encountered a blunt dissection in combination with an iodine solution to simulate a nerve injury. Subsequently, the regeneration process and drug administration efficiency could be monitored. Moreover, this method is successfully performed to detect nerve injury and quantitatively calculate microcirculation in injured peripheral nerves (79). In addition to mentioned diseases, high-resolution ultrasound is an appropriate device to determine Schwannomas, solid tumors in peripheral nerve, with the sign of hypoechoic signals and neurofibromas, mainly in the subcutaneous tissue, with the hyperechoic area along with neurofibromatosis 1 and 2 (80). The US combined with MR neurography resulted in high-resolution peripheral nerve imaging, which covers the detection of a wide range of nerve lesions as well as (non)focal neuropathies (81) (Figure 2).

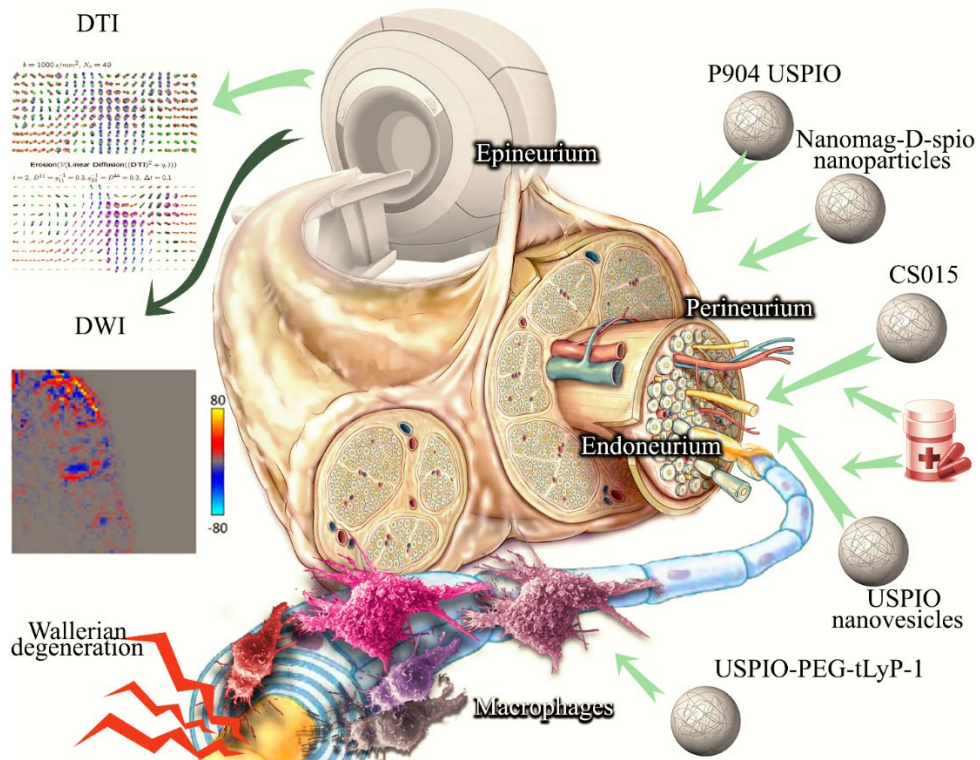


Figure 1. The suggested application of the USPIO nanoparticles in peripheral nerve imaging and tracking is depicted along with potential imaging techniques such as DWI, DTI, and T₂* mapping

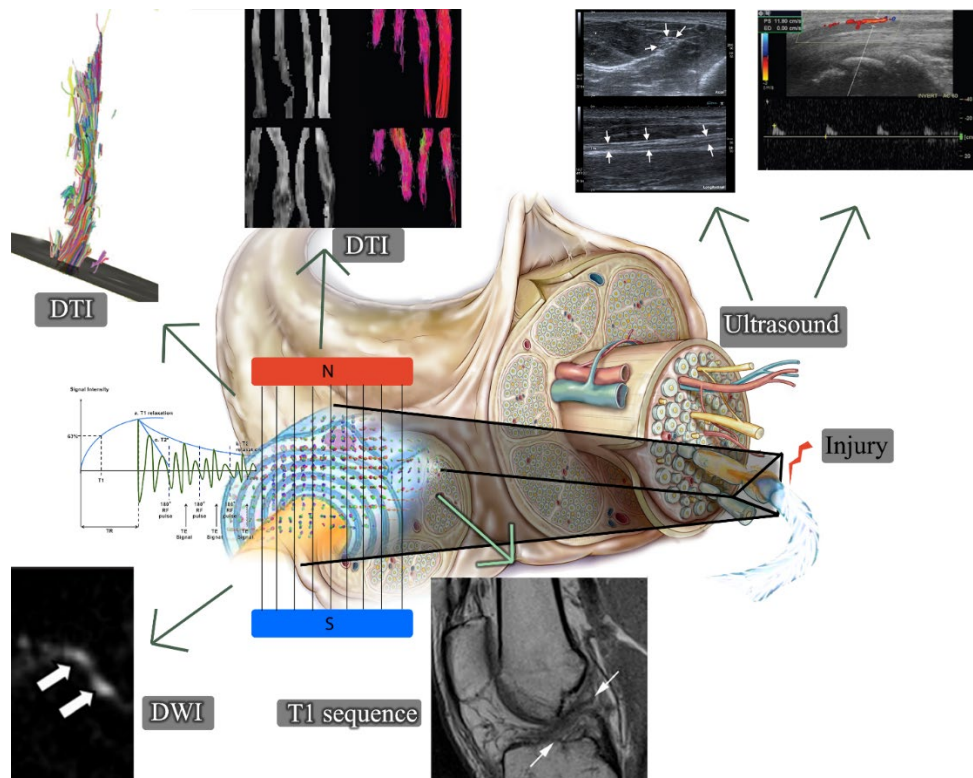


Figure 2. An overview of the nerve injury diagnosis, using some practical MRI sequences and Ultrasound

Discussion

In the current review, there was a particular focus on the clinical approaches in PNS imaging, along with

discussing contrast agents and introducing MRI sequences. Our study's main finding and novelty is

synopsized into the applicable role of the DTI method, especially the FA value in evaluating the structural health of the PNS. These results suggest a new candidate for diagnostic approaches that benefits surgeons and physicians, while currently PNS evaluation is implemented with the aid of electromyography (EMG) and nerve conduction studies (NCS) (82).

In a recent review article conducted by Endo et al., the MRI was signified as a mighty method in detecting the denervation of the superficial and deep nerves (83). Accordingly, in our study, the DTI method as one of the MRI sequences, was suggested as the suitable option to make an accurate diagnosis of denervation and other types of physical nerve injuries. Furthermore, in a systematic review evaluating the role of DTI in acquiring data about the brachial plexus, the results mentioned two values of FA and MD as the diagnostic parameters for detecting the changes in the quality of the nerves (84). Likewise, in our study, the value of FA was sensitive to denervation, while the value of MD was a proper parameter in monitoring nerve regeneration. More specifically, in a review article written by Martín et al., the FA value in revealing neuropathy in which the FA value reduces, was on the debate. The author continued by pointing out the downward trend of the FA value in the PNS injury. To provide supplementary information regarding the previous result, the role of RD in evaluating the myelination integrity of the nerves, along with the quality of the connective tissue was commented on, in which the remyelination procedure could be validated by observing a reduction in the RD value. In addition to the DTI property in the detection of nerve malformations, the cited review article briefly mentioned the role of the conventional MRI in the detection of nerve injuries, by stating fast spin-echo and TSE sequences along with fat suppression, as the validated methods to evaluate PNS (58). Accordingly, the main deduction of our study consisting of six original articles evaluating the DTI methods, was in line with Martín et al. study. In addition, Martín explanation of the role of conventional MRI was similar to our interpretation as well as Filler et al. (37) and Moser et al. (38) results. In addition to the beneficial role of MRI, it is worth mentioning the controversial issues about MRI corresponding to the DWI roles, in detecting MPNST and pNF. Accordingly, in a review article conducted by Donaldson et al., the author reported that MRI cannot determine MPNST since among the MRI taken from three patients, only one was suspected of tumor presence, without providing data about tumor type (85).

Besides the MRI technique, in a review article mentioning the role of ultrasonography in PNS imaging, multiple benefits were indicated. Accordingly, the ability of the ultrasound to track and rate the grade of the nerve injury, was supposed to be a practical technique for surgery operations (86).

Similarly, in the current study, the role of ultrasonography and its accuracy in the detection of MPNST and BPNSTs has been briefly mentioned. Although the role of ultrasonography was highlighted in monitoring the nerve regeneration process, MRI advanced techniques have superiority over its in demonstrating nerve injury. The declaration of the priority of the MRI technique over ultrasonography, relies on the low contrast of ultrasonography. In support of this issue, Jerban et al. systematic review could be mentioned, which specified the low contrast and artifact as the main limitations of ultrasonography (87). Correspondingly, in a review article demonstrating the advances in MRI technology, DTI has been introduced as a potent method in determining the grade of nerve injury with a high spatial resolution (88).

Conclusion

Peripheral nerve injuries have many subunits, which cause difficulty in proper diagnosis and using suitable therapeutic methods. These difficulties are due to the complicated procedure of imaging and several issues in implementing the traditional MRI method, including the isointense signal of muscles, nerves, and vessels in T1 weighted sequences as well as the same appearance in diameter of the vessels and nerves (39, 45, 46). Nonetheless, thanks to advanced imaging techniques, most of these challenges have been overcome. To compensate for the isointense issue, contrast agents and USPIOs particles are applied to the targeted tissue. Accordingly, USPIO nanovesicles, nanoparticles, and P904 USPIOs could be utilized to provide suitable contrast, in order to differentiate nerves from adjacent tissue (33, 35). Moreover, with the aid of USPIOs, drug delivery could be tracked, and immune cells could be marked to visualize minor nerve inflammation (30, 31). In addition to USPIOs, the image contrast in specifying PNS is improved by some basic manipulation on echo time, TR, and TE, resulting in gathering of different sequences like SE or TSE sequences. Alternatively, a combination of methods including STIR and T1 weighted sequences, along with gadolinium injection may be applied to get high-quality images (37, 38). Apart from the contrast issue, in the PNS image acquisition, artifacts that deteriorate in high MFS, mislead the physician for making a reasonable deduction. For instance, in the DTI and 3D DW-PSIF sequences, artifacts disrupt some proportion of the PNS details. As an alternative, the msEPI-SPiR sequence and TOPUP image recovering tool for DTI sequencing, could be applied to decrease the artifact effects (62, 67). Another challenge in the clinical application of PNS is the conflicting interpretation of the data. In this regard, some hallmarks would be utilized in signified malady conditions, such as an increase in nerve root diameter that is as an indication of inflammatory polyneuropathies (40). Besides, in the DTI sequence, a reduction in the FA parameter, illustrated the myelin and axon degeneration and the alternation in the MD

value, provided a quantitative scale for nerve recovery (69).

Finally, the dynamic and live evaluation of the PNS is one of the requirements for the accurate diagnosis of PNS diseases. Among imaging instruments, fMRI and sonography are gathering dynamics images. Sonography lacks the minimum contrast quality to visualize details, while by utilizing fMRI, even microstructural changes could be revealed (57, 79) (Fig2).

Acknowledgments

This work is supported by Iran University of Medical Sciences.

Funding

The authors did not receive any funding.

Authors' contributions

Auob Rustamzadeh contributes to the study concept and design. Armin Ariaei contributes to data acquisition and writing. Mehran Ebrahimi Shah-abadi, Arash Shabani, Hossein Mohammadi, Rastegar Rahmani Tanha, Vahid Tavakolian Ferdousie, and Mohsen Marzban contribute to reviewing and editing. Abdolmajid Taheri and Mahdi Heydari contribute to revising the article. All authors read and approved the final manuscript.

Data availability

This review article contains no supplementary or raw data.

Conflict of Interest

There is no conflict of interest.

References

- Ohana M, Moser T, Moussaoui A, et al. Current and future imaging of the peripheral nervous system. *Diag Intervent Imag.* 2014;95(1):17-26. [DOI:10.1016/j.diii.2013.05.008] [PMID]
- Möller I, Miguel M, Bong DA, Zaottini F, Martinoli C. The peripheral nerves: update on ultrasound and magnetic resonance imaging. *Clin Exp Rheumatol.* 2018;36(Suppl 114):145-58.
- Piña-Oviedo S, Ortiz-Hidalgo C. The normal and neoplastic perineurium: a review. *Adv Anat Pathol.* 2008;15(3):147-64. [DOI:10.1097/PAP.0b013e31816f8519] [PMID]
- Planitzer U, Steinke H, Meixensberger J, Bechmann I, Hammer N, Winkler D. Median nerve fascicular anatomy as a basis for distal neural prostheses. *Ann Anat.* 2014;196(2-3):144-9. [DOI:10.1016/j.aanat.2013.11.002] [PMID]
- Stewart JD. Peripheral nerve fascicles: anatomy and clinical relevance. *Muscle Nerve.* 2003;28(5):525-41. [DOI:10.1002/mus.10454] [PMID]
- Danafar H, Baghdadchi Y, Barsbay M, Ghaffarlou M, Mousazadeh N, Mohammadi A. Synthesis of Fe(3)O(4)-gold hybrid nanoparticles coated by bovine serum albumin as a contrast agent in MR imaging. *Heliyon.* 2023;9(3):e13874. [PMCID] [DOI:10.1016/j.heliyon.2023.e13874] [PMID]
- Khosravi H, Doosti-Irani A, Bouraghi H, Nikzad S. Investigation of gold nanoparticles effects in radiation therapy of cancer: A systematic review. *J Adv Med Biomed Res.* 2022;30(142):388-96. [DOI:10.30699/jambs.30.142.1]
- Maddah A, Ziamajidi N, Khosravi H, Danesh H, Abbasalipourkabir R. Gold nanoparticles induce apoptosis in HCT-116 colon cancer cell line. *Molec Biol Rep.* 2022;49(8):7863-71. [DOI:10.1007/s11033-022-07616-6] [PMID]
- Khosravi H, Hashemi B, Mahdavi SR, Hejazi P. Target dose enhancement factor alterations related to interaction between the photon beam energy and gold nanoparticles size in external radiotherapy: using monte carlo method. *Koomeh.* 2015;17(1):255-61.
- Khosravi H, Mahdavi A, Rahmani F, Ebadi A. The impact of nano-sized gold particles on the target dose enhancement based on photon beams using by monte carlo method. *Nanomed Res J.* 2016;1(2):84-9.
- Sayyed M, Hamad MK, Mhareb M, Prabhu NS, Khosravi H, Kamath SD. Effect of different modifiers on mechanical and radiation shielding properties of SrO-B2O3-TeO2 glass system. *Optik.* 2022;257:168823. [DOI:10.1016/j.ijleo.2022.168823]
- Zhang K, Jiang M, Fang Y. The drama of Wallerian degeneration: the cast, crew, and script. *Ann Rev Genet.* 2021;55:93-113. [PMID] [DOI:10.1146/annurev-genet-071819-103917]
- Arthur-Farraj P, Coleman MP. Lessons from injury: How nerve injury studies reveal basic biological mechanisms and therapeutic opportunities for peripheral nerve diseases. *Neurotherapeut.* 2021:1-22. [PMID] [PMCID] [DOI:10.1007/s13311-021-01125-3]
- Gaudet AD, Popovich PG, Ramer MS. Wallerian degeneration: gaining perspective on inflammatory events after peripheral nerve injury. *J Neuroinflamm.* 2011;8(1):1-13. [PMCID] [DOI:10.1186/1742-2094-8-110] [PMID]
- Zigmond RE, Echevarria FD. Macrophage biology in the peripheral nervous system after injury. *Prog*

- Neurobiol. 2019;173:102-21. [PMID] [PMCID] [DOI:10.1016/j.pneurobio.2018.12.001]
16. Cattin AL, Burden JJ, Van Emmenis L, et al. Macrophage-induced blood vessels guide Schwann cell-mediated regeneration of peripheral nerves. *Cell*. 2015;162(5):1127-39. [PMCID] [DOI:10.1016/j.cell.2015.07.021] [PMID]
 17. Bombeiro AL, Pereira BTN, de Oliveira ALR. Granulocyte-macrophage colony-stimulating factor improves mouse peripheral nerve regeneration following sciatic nerve crush. *Europ J Neurosci*. 2018;48(5):2152-64. [DOI:10.1111/ejn.14106] [PMID]
 18. Stratton JA, Holmes A, Rosin NL, et al. Macrophages regulate Schwann cell maturation after nerve injury. *Cell Rep*. 2018;24(10):2561-72.e6. [DOI:10.1016/j.celrep.2018.08.004] [PMID]
 19. Jack MM, Smith BW, Spinner RJ. Neurosurgery for the neurologist: Peripheral nerve injury and compression (What can be Fixed?). *Neurol Clin*. 2022;40(2):283-95. [DOI:10.1016/j.ncl.2021.11.001] [PMID]
 20. Shores JT, Malek V, Lee WA, Brandacher G. Outcomes after hand and upper extremity transplantation. *J Mater Sci Mater Med*. 2017;28:1-8. [DOI:10.1007/s10856-017-5880-0] [PMID]
 21. Wolford LM, Stevao EL. Considerations in nerve repair. *Proc (Bayl Univ Med Cent)*. 2003;16(2):152-6. [DOI:10.1080/08998280.2003.11927897] [PMID] [PMCID]
 22. Kong FL, Bie ZX, Wang Z, Peng JZ, Li XG. Nerve injury and regeneration after neurolysis: ethanol alone versus ethanol with brachytherapy in rabbits. *J Vasc Interv Radiol*. 2022;33(9):1066-1072.e1 [DOI:10.1016/j.jvir.2022.06.006] [PMID]
 23. Charoenlux P, Utoomprurkporn N, Seresirikachorn K. The efficacy of corticosteroid after facial nerve neurolysis: a systematic review and meta-analysis of randomized controlled trial. *Brazil J Otorhinolaryngol*. 2023;89:79-89. [DOI:10.1016/j.bjorl.2021.09.005] [PMID] [PMCID]
 24. Yoshioka N. Partial hypoglossal-facial end-to-end neurolysis for nonflaccid facial palsy with severe hypertonicity. *Interdiscipl Neurosurg*. 2022;28:101484. [DOI:10.1016/j.inat.2021.101484]
 25. Dadfar SM, Roemhild K, Drude NI, et al. Iron oxide nanoparticles: Diagnostic, therapeutic and theranostic applications. *Adv Drug Deliver Rev*. 2019;138:302-25. [PMID] [PMCID] [DOI:10.1016/j.addr.2019.01.005]
 26. Zhao Y, Zhao X, Cheng Y, Guo X, Yuan W. Iron oxide nanoparticles-based vaccine delivery for cancer treatment. *Molec Pharmaceut*. 2018;15(5):1791-9. [PMID] [DOI:10.1021/acs.molpharmaceut.7b01103]
 27. Bjørnerud A, Johansson L. The utility of superparamagnetic contrast agents in MRI: theoretical consideration and applications in the cardiovascular system. *NMR Biomed*. 2004;17(7):465-77. [DOI:10.1002/nbm.904] [PMID]
 28. Maraloiu VA, Appaix F, Broisat A, et al. Multiscale investigation of USPIO nanoparticles in atherosclerotic plaques and their catabolism and storage in vivo. *Nanomedicine*. 2016;12(1):191-200. [DOI:10.1016/j.nano.2015.08.005] [PMID]
 29. Oghabian MA, Gharehaghaji N, Amirmohseni S, Khoei S, Guiti M. Detection sensitivity of lymph nodes of various sizes using USPIO nanoparticles in magnetic resonance imaging. *Nanomedicine*. 2010;6(3):496-9. [DOI:10.1016/j.nano.2009.11.005] [PMID]
 30. Nie Y, Rui Y, Miao C, Li Q, Hu F, Gu H. A stable USPIO capable for MR lymphography with Ultra-low effective dosage. *Nanomedicine*. 2020;29:102233. [DOI:10.1016/j.nano.2020.102233] [PMID]
 31. Wu W, Zhong S, Gong Y, et al. A new molecular probe: an NRP-1 targeting probe for the grading diagnosis of glioma in nude mice. *Neurosci Lett*. 2020;714:134617. [DOI:10.1016/j.neulet.2019.134617] [PMID]
 32. Liu Q, Chen S, Hao L, et al. Preparation of fluorescent bimodal probe coupled with ultra-small superparamagnetic iron oxide particles. *J Radiat Res App Sci*. 2022;15(2):143-8. [DOI:10.1016/j.jrras.2022.04.009]
 33. Xie T, Chen X, Fang J, et al. Non-invasive monitoring of the kinetic infiltration and therapeutic efficacy of nanoparticle-labeled chimeric antigen receptor T cells in glioblastoma via 7.0-Tesla magnetic resonance imaging. *Cytotherapy*. 2021;23(3):211-22. [DOI:10.1016/j.jcyt.2020.10.006] [PMID]
 34. Hu Q, Cao H, Zhou L, et al. Measurement of BAT activity by targeted molecular magnetic resonance imaging. *Magnet Resonance Imag*. 2021;77:1-6. [DOI:10.1016/j.mri.2020.12.006] [PMID]
 35. Liu D, Zhou Z, Wang X, et al. Yolk-shell nanovesicles endow glutathione-responsive concurrent drug release and T1 MRI activation for cancer theranostics. *Biomaterials*. 2020;244:119979. [PMID] [PMCID] [DOI:10.1016/j.biomaterials.2020.119979]
 36. Kim S, Choi JY, Huh YM, et al. Role of magnetic resonance imaging in entrapment and compressive neuropathy-what, where, and how to see the peripheral nerves on the musculoskeletal magnetic resonance image: part 2. Upper extremity. *Europ*

- Radiol. 2007;17(2):509-22.
[DOI:10.1007/s00330-006-0180-y] [PMID]
37. Filler AG, Maravilla KR, Tsuruda JS. MR neurography and muscle MR imaging for image diagnosis of disorders affecting the peripheral nerves and musculature. *Neurol Clin.* 2004;22(3):643-82. [DOI:10.1016/j.ncl.2004.03.005] [PMID]
 38. Moser T, Kremer S, Holl N. Imaging of the peripheral nerve: anatomy, exploration techniques and main pathologies. *J Radiol.* 2009; 90(10):1448. [DOI:10.1016/S0221-0363(09)75678-1]
 39. Deroide N, Bousson V, Lévy BI, Laredo JD, Kubis N. Nerve and muscle imaging in peripheral nerve damage associated with electroneuromyography: the ideal couple? *J Int Med.* 2010; 31(4):287-94. [DOI:10.1016/j.revmed.2009.03.021] [PMID]
 40. Mulkey SB, Glasier CM, El-Nabbout B, et al. Nerve root enhancement on spinal MRI in pediatric Guillain-Barré syndrome. *Pediatr Neurol.* 2010;43(4):263-9. [PMID] [DOI:10.1016/j.pediatrneurol.2010.05.011]
 41. Stanisiz GJ, Midha R, Munro CA, Henkelman RM. MR properties of rat sciatic nerve following trauma. *Magnet Reson Med.* 2001;45(3):415-20. [DOI:10.1002/1522-2594(200103)45:33.0.CO;2-M] [PMID]
 42. Bendszus M, Wessig C, Solymosi L, Reiners K, Koltzenburg M. MRI of peripheral nerve degeneration and regeneration: correlation with electrophysiology and histology. *Experiment Neurol.* 2004;188(1):171-7. [DOI:10.1016/j.expneurol.2004.03.025] [PMID]
 43. Bendszus M, Koltzenburg M, Wessig C, Solymosi L. Sequential MR imaging of denervated muscle: experimental study. *Am J Neuroradiol.* 2002; 23(8):1427-31.
 44. Kamath S, Venkatanarasimha N, Walsh M, Hughes P. MRI appearance of muscle denervation. *Skelet Radiol.* 2008;37(5):397-404. [DOI:10.1007/s00256-007-0409-0] [PMID]
 45. Chhabra A, Soldatos T, Subhawong TK, et al. The application of three-dimensional diffusion-weighted PSIF technique in peripheral nerve imaging of the distal extremities. *J Magnet Reson Imag.* 2011;34(4):962-7. [DOI:10.1002/jmri.22684] [PMID]
 46. Chhabra A, Subhawong TK, Bizzell C, Flammang A, Soldatos T. 3T MR neurography using three-dimensional diffusion-weighted PSIF: technical issues and advantages. *Skelet Radiol.* 2011; 40(10):1355-60. [PMID] [DOI:10.1007/s00256-011-1162-y]
 47. Chhabra A, Soldatos T, Flammang A, Gilson W, Padua A, Carrino JA. 3T MR imaging of peripheral nerves using 3D diffusion-weighted PSIF technique. 2010.
 48. Freund W, Brinkmann A, Wagner F, et al. MR neurography with multiplanar reconstruction of 3D MRI datasets: an anatomical study and clinical applications. *Neuroradiol.* 2007;49(4):335-41. [DOI:10.1007/s00234-006-0197-6] [PMID]
 49. Viallon M, Vargas M, Jlassi H, Lövblad KO, Delavelle J. High-resolution and functional magnetic resonance imaging of the brachial plexus using an isotropic 3D T2 STIR (Short Term Inversion Recovery) SPACE sequence and diffusion tensor imaging. *Europ Radiol.* 2008; 18(5):1018-23. [PMID] [DOI:10.1007/s00330-007-0834-4]
 50. Zare M, Faeghi F, Hosseini A, Ardekani MS, Heidari MH, Zarei E. Comparison between three-dimensional diffusion-weighted PSIF technique and routine imaging sequences in evaluation of peripheral nerves in healthy people. *Basic Clin Neurosci.* 2018;9(1):65. [PMID] [PMCID] [DOI:10.29252/nirp.bcn.9.1.65]
 51. Tereshenko V, Pashkunova-Martic I, Manzano-Szalai K, et al. MR imaging of peripheral nerves using targeted application of contrast agents: An experimental proof-of-concept study. *Front Med.* 2020;7:613138. [PMID] [PMCID] [DOI:10.3389/fmed.2020.613138]
 52. Bendszus M, Stoll G. Caught in the act: in vivo mapping of macrophage infiltration in nerve injury by magnetic resonance imaging. *J Neurosci.* 2003; 23(34):10892-6. [DOI:10.1523/JNEUROSCI.23-34-10892.2003] [PMID] [PMCID]
 53. Bendszus M, Wessig C, Schütz A, et al. Assessment of nerve degeneration by gadofluorine M-enhanced magnetic resonance imaging. *Ann Neurol.* 2005;57(3):388-95. [DOI:10.1002/ana.20404] [PMID]
 54. Kobayashi S, Meir A, Baba H, Uchida K, Hayakawa K. Imaging of intraneural edema by using gadolinium-enhanced MR imaging: experimental compression injury. *Am J Neuroradiol.* 2005;26(4):973-80.
 55. Bouldin TW, Earnhardt TS, Goines ND. Restoration of blood-nerve barrier in neuropathy is associated with axonal regeneration and remyelination. *J Neuropathol Exp Neurol.* 1991; 50(6):719-28. [PMID] [DOI:10.1097/00005072-199111000-00004]
 56. Omura K, Ohbayashi M, Sano M, Omura T, Hasegawa T, Nagano A. The recovery of blood-nerve barrier in crush nerve injury—a quantitative analysis utilizing immunohistochemistry. *Brain Res.* 2004;1001(1-2):13-21. [DOI:10.1016/j.brainres.2003.10.067] [PMID]

57. Spees WM, Lin TH, Sun P, et al. MRI-based assessment of function and dysfunction in myelinated axons. *Proc Nat Acad Sci USA*. 2018; 115(43):E10225-E34. [PMID] [PMCID] [DOI:10.1073/pnas.1801788115]
58. Martín Noguero T, Barousse R, Gómez Cabrera M, Socolovsky M, Bencardino JT, Luna A. Functional MR neurography in evaluation of peripheral nerve trauma and postsurgical assessment. *Radiograph*. 2019;39(2):427-46. [DOI:10.1148/rg.2019180112] [PMID]
59. de Figueiredo EH, Borgonovi AF, Doring TM. Basic concepts of MR imaging, diffusion MR imaging, and diffusion tensor imaging. *Magn Reson Imaging Clin N Am*. 2011;19(1):1-22. [DOI:10.1016/j.mric.2010.10.005] [PMID]
60. De Vuysere S, Vandecaveye V, De Bruecker Y, et al. Accuracy of whole-body diffusion-weighted MRI (WB-DWI/MRI) in diagnosis, staging and follow-up of gastric cancer, in comparison to CT: a pilot study. *BMC Med Imag*. 2021;21(1):1-9. [DOI:10.1186/s12880-021-00550-2] [PMID] [PMCID]
61. Takahara T, Hendrikse J, Kwee TC, et al. Diffusion-weighted MR neurography of the sacral plexus with unidirectional motion probing gradients. *Eur Radiol*. 2010;20(5):1221-6. [DOI:10.1007/s00330-009-1665-2] [PMID] [PMCID]
62. Bae YJ, Choi BS, Jeong HK, Sunwoo L, Jung C, Kim JH. Diffusion-weighted imaging of the head and neck: Influence of fat-suppression technique and multishot 2D navigated interleaved acquisitions. *AJNR Am J Neuroradiol*. 2018; 39(1):145-50. [DOI:10.3174/ajnr.A5426] [PMID] [PMCID]
63. Takahara T, Hendrikse J, Yamashita T, et al. Diffusion-weighted MR neurography of the brachial plexus: feasibility study. *Radiol*. 2008; 249(2):653-60. [DOI:10.1148/radiol.2492071826] [PMID]
64. Koike H, Nishida Y, Ito S, et al. Diffusion-weighted magnetic resonance imaging improves the accuracy of differentiation of benign from malignant peripheral nerve sheath tumors. *World Neurosurg*. 2022;157:e207-e14. [DOI:10.1016/j.wneu.2021.09.130] [PMID]
65. Haakma W, Dik P, ten Haken B, et al. Diffusion tensor magnetic resonance imaging and fiber tractography of the sacral plexus in children with spina bifida. *J Urol*. 2014;192(3):927-33. [DOI:10.1016/j.juro.2014.02.2581] [PMID]
66. Farinas AF, Esteve IVM, Pollins AC, et al. Diffusion MRI predicts peripheral nerve recovery in a rat sciatic nerve injury model. *Plast Reconstruct Surg*. 2020;145(4):949. [PMCID] [DOI:10.1097/PRS.0000000000006638] [PMID]
67. Schmid AB, Campbell J, Hurley SA, et al. Feasibility of diffusion tensor and morphologic imaging of peripheral nerves at ultra-high field strength. *Investig Radiol*. 2018;53(12):705. [DOI:10.1097/RLI.0000000000000492] [PMID] [PMCID]
68. Chiang CW, Wang Y, et al. Quantifying white matter tract diffusion parameters in the presence of increased extra-fiber cellularity and vasogenic edema. *Neuroimage*. 2014;101:310-9. [PMCID] [DOI:10.1016/j.neuroimage.2014.06.064] [PMID]
69. Sun C, Hou Z, Hong G, Wan Q, Li X. In vivo evaluation of sciatic nerve crush injury using diffusion tensor imaging: correlation with nerve function and histology. *J Comput Assist Tomograph*. 2014;38(5):790-6. [DOI:10.1097/RCT.0000000000001035] [PMID]
70. Yamasaki T, Fujiwara H, Oda R, et al. In vivo evaluation of rabbit sciatic nerve regeneration with diffusion tensor imaging (DTI): correlations with histology and behavior. *Magnet Reson Imag*. 2015;33(1):95-101. [DOI:10.1016/j.mri.2014.09.005] [PMID]
71. Heckel A, Weiler M, Xia A, et al. Peripheral nerve diffusion tensor imaging: assessment of axon and myelin sheath integrity. *PLoS One*. 2015;10(6):e0130833. [DOI:10.1371/journal.pone.0130833] [PMID] [PMCID]
72. de Noordhout AM. Usefulness of ultrasonography, MRI and CT scan in the diagnosis of entrapment neuropathies. *Rev Neurol (Paris)*. 2007;163(12):1263-5. [DOI:10.1016/S0035-3787(07)78417-5] [PMID]
73. Pilavaki M, Chourmouzi D, Kiziridou A, Skordalaki A, Zarampoukas T, Drevelengas A. Imaging of peripheral nerve sheath tumors with pathologic correlation: pictorial review. *Eur J Radiol*. 2004;52(3):229-39. [DOI:10.1016/j.ejrad.2003.12.001] [PMID]
74. Mandalà S, Lupo M, Guccione M, La Barbera C, Iadicola D, Mirabella A. Small bowel gastrointestinal stromal tumor presenting with gastrointestinal bleeding in patient with type 1 Neurofibromatosis: Management and laparoscopic treatment. Case report and review of the literature. *Int J Surg Case Rep*. 2021;79:84-90. [DOI:10.1016/j.ijscr.2020.12.095] [PMID] [PMCID]
75. Rimeika G, Saba L, Arthimulam G, et al. Metanalysis on the effectiveness of low back pain treatment with oxygen-ozone mixture: Comparison between image-guided and non-image-guided injection techniques. *Europ J Radiol*

- Open. 2021;8:100389. [PMID] [PMCID] [DOI:10.1016/j.ejro.2021.100389]
76. Koob M, Dietemann JL. Imaging of peripheral lesions of type 1 neurofibromatosis. *J Radiol.* 2009;90(10):1448-9. [DOI:10.1016/S0221-0363(09)75679-3]
 77. Yan D, Jiman AA, Bottorff EC, et al. Ultraflexible and stretchable intrafascicular peripheral nerve recording device with axon-dimension, cuff-less microneedle electrode array. *Small.* 2022: 2200311. [DOI:10.1101/2022.01.19.476928]
 78. Jin Z, Zhao K, Guo W, Wang D, Deng Y, Chen T. Investigation of ultrasound parameters for the differential diagnosis of malignant and benign peripheral nerve sheath tumors. *J Ultrasound Med.* 2022. [DOI:10.1002/jum.16089] [PMID]
 79. Zhu Y, Jin Z, Wang J, et al. Ultrasound-guided platelet-rich plasma injection and multimodality ultrasound examination of peripheral nerve crush injury. *NPJ Regenerat Med.* 2020;5(1):1-13. [DOI:10.1038/s41536-020-00101-3] [PMID] [PMCID]
 80. Winter N, Dohrn MF, Wittlinger J, Loizides A, Gruber H, Grimm A. Role of high-resolution ultrasound in detection and monitoring of peripheral nerve tumor burden in neurofibromatosis in children. *Child Nerv Syst.* 2020;36(10):2427-32. [PMID] [PMCID] [DOI:10.1007/s00381-020-04718-z]
 81. Pham M, Bäumer T, Bendszus M. Peripheral nerves and plexus: imaging by MR-neurography and high-resolution ultrasound. *Curr Opin Neurol.* 2014;27(4):370-9. [PMID] [DOI:10.1097/WCO.000000000000111]
 82. Kamble N, Shukla D, Bhat D. Peripheral nerve injuries: Electrophysiology for the neurosurgeon. *Neurol India.* 2019;67(6):1419-22. [DOI:10.4103/0028-3886.273626] [PMID]
 83. Endo Y, Miller TT, Sneag DB. Imaging of the peripheral nerves of the lower extremity. *Radiol Clin North Am.* 2023;61(2):381-92. [DOI:10.1016/j.rcl.2022.10.011] [PMID]
 84. Wade RG, Whittam A, Teh I, et al. Diffusion tensor imaging of the roots of the brachial plexus: a systematic review and meta-analysis of normative values. *Clin Transl Imag.* 2020;8(6): 419-31. [DOI:10.1007/s40336-020-00393-x] [PMID] [PMCID]
 85. Donaldson EK, Winter JM, Chandler RM, Clark TA, Giuffre JL. Malignant peripheral nerve sheath tumors of the brachial plexus: A single-center experience on diagnosis, management, and outcomes. *Ann Plast Surg.* 2023;90(4):339-42. [DOI:10.1097/SAP.0000000000003462] [PMID]
 86. Samet JD. Ultrasound of peripheral nerve injury. *Pediatr Radiol.* 2023. [DOI:10.1007/s00247-023-05631-8] [PMID]
 87. Jerban S, Barrère V, Andre M, Chang EY, Shah SB. Quantitative Ultrasound Techniques Used for Peripheral Nerve Assessment. *Diagnostics (Basel).* 2023;13(5). [PMID] [PMCID] [DOI:10.3390/diagnostics13050956]
 88. Sneag DB, Queler S. Technological Advancements in Magnetic Resonance Neurography. *Curr Neurol Neurosci Rep.* 2019; 19(10):75. [DOI:10.1007/s11910-019-0996-x] [PMID]

How to Cite This Article:

Ebrahimi Shah-abadi M, Ariaei A, Mohammadi H, Shabani A, Rahmani Tanha R, Tavakolian Ferdousie V, et al. Recent Advances and Future Directions in Imaging of Peripheral Nervous System: A Comprehensive Review for Therapeutics Approach. *J Adv Med Biomed Res.* 2023; 31(138):415-31.

Download citation:

[BibTeX](#) | [RIS](#) | [EndNote](#) | [Medlars](#) | [ProCite](#) | [Reference Manager](#) | [RefWorks](#)

Send citation to:

 [Mendeley](#)  [Zotero](#)  [RefWorks](#) [RefWorks](#)